UKAEA-CCFE-PR(20)100

V.G. Kiptily, M. Fitzgerald, Ye.O. Kazakov, M. Nocente, J. Ongena, S.E. Sharapov, M. Dreval, Ž. Štancar, T. Craciunescu, J. Garcia, L. Giacomelli, V.Goloborodko, J. Oliver, H. Weisen

Evidence for Alfvén Eigenmodes Driven by Alpha Particles in D-3He Fusion Experiments on JET

Evidence for Alfvén Eigenmodes Driven by Alpha Particles in D-3He Fusion Experiments on JET

V.G. Kiptily, M. Fitzgerald, Ye.O. Kazakov, M. Nocente, J. Ongena, S.E. Sharapov, M. Dreval, Ž. Štancar, T. Craciunescu, J. Garcia, L. Giacomelli, V.Goloborodko, J. Oliver, H. Weisen

This is a preprint of a paper submitted for publication in
Nuclear Fusion Letter

Evidence for Alfvén Eigenmodes Driven by Alpha Particles in D-^{3}He Fusion Experiments on JET

V.G. Kiptily[1], M. Fitzgerald[1], Ye.O. Kazakov[2], M. Nocente[3,4], J. Ongena[2],
S.E. Sharapov[1], M. Dreval[5], Ž. Štancar[6], T. Craciunescu[7], J. Garcia[8],
L. Giacomelli[4], V. Goloborodko[9], H.J.C. Oliver[1], H. Weisen[10] and JET Contributors*

[1] CCFE, Culham Science Centre, Abingdon, UK
[2] Laboratory for Plasma Physics, LPP-ERM/KMS, TEC Partner, Brussels, Belgium
[3] Dipartimento di Fisica, Università di Milano-Bicocca, Milan, Italy
[4] Institute for Plasma Science and Technology, National Research Council, Milan, Italy
[5] National Science Centre 'Kharkiv Institute of Physics and Technology', Kharkiv, Ukraine
[6] Jožef Stefan Institute, Ljubljana, Slovenia
[7] National Institute for Laser, Plasma and Radiation Physics, Bucharest, Romania
[8] CEA, IRFM, Saint-Paul-lez-Durance, France
[9] KINR, Kyiv, Ukraine
[10] EPFL, Swiss Plasma Centre (SPC), Lausanne, Switzerland

** See the author list of "Overview of the JET preparation for Deuterium-Tritium Operation" by E. Joffrin et al., Nucl. Fusion **59**, 112021 (2019)*

Abstract

Dedicated experiments to generate high-energy D ions and D-^{3}He fusion-born alpha particles have been performed at the Joint European Torus (JET) with the ITER-like wall (ILW). Deuterium ions from neutral beam injection (NBI) with acceleration voltage of 100 keV were accelerated to higher energies in the core of mixed D-^{3}He plasmas by applying the 3-ion radio frequency (RF) scenario. A large variety of fast-ion driven magnetohydrodynamic (MHD) modes with different toroidal mode numbers n were observed in these JET-ILW experiments, including the $n = -1$ and $n = 0$ modes in the frequency range of the elliptical Alfvén eigenmodes (EAEs). The simultaneous observation of these modes implies the presence of a fast-ion population in the plasma with a large number of highly energetic counter-passing ions, in addition to having a positive gradient in the particle energy distribution function. The combined fast-ion and MHD analysis shows that the population of RF-generated fast D ions does not include particles capable to excite effectively $n = -1$ EAEs. We demonstrate that the fast-ion observations are consistent with the hypothesis that D-^{3}He fusion-born alpha particles are the drive for these modes. For the first time, we propose a theoretical mechanism and provide experimental evidence for a bump-on-tail distribution of fusion-born alphas required to excite $n = 0$ AEs, self-sustained by a periodic modulation of the fusion source due to sawtooth crashes.

Introduction

In a thermonuclear fusion reactor, the reaction between deuterium (D) and tritium (T) ions, resulting in a fast alpha particle (^{4}He) and a neutron, will be the main source of energy

$$\mathrm{D} + \mathrm{T} \rightarrow {}^4\mathrm{He}\ (3.5\ \mathrm{MeV}) + n\ (14.1\ \mathrm{MeV}). \tag{1}$$

The concept of magnetic confinement crucially relies on self-heating by fusion-born alpha particles. To this end, the alpha particles must be well confined to transfer their energy to the plasma particles during their collisional slowing-down. Equally important is that additional effects associated with the presence of the alpha particles do not lead to a detrimental degradation of the plasma confinement. Among these, the excitation and interaction of alpha particles with magnetohydrodynamic (MHD) modes is of particular importance for the development of magnetic fusion reactors. Indeed, consequences on fast ion transport and confinement can be substantial and the Alfvén instability is a significant issue for high-Q operation in ITER [1]. Therefore, dedicated alpha particle studies were undertaken in past D-T experiments on the TFTR and JET tokamaks [2, 3]. Further alpha physics studies are planned in the forthcoming D-T campaign in JET with the ITER-like wall (JET-ILW) [4].

Effects from fusion-born alpha particles can be studied in JET-ILW before the planned full-scale D-T experiments, characterized using tritium and harsh radiation conditions for diagnostics. These studies rely on generating fast alpha particles using the reaction between D and ^{3}He ions, which does not produce neutrons

$$\mathrm{D} + {}^3\mathrm{He} \rightarrow {}^4\mathrm{He}\ (3.6\ \mathrm{MeV}) + p\ (14.7\ \mathrm{MeV}), \tag{2}$$

however, the birth energy and kinematics of alpha particles from this reaction are very close to those released in D-T reactions [5] and the transport in the plasma is the same. In JET-ILW, the toroidal magnetic field (B_t) and plasma current (I_p) are oriented in the same direction (clockwise if viewed from the top of the machine). In the studies reported in this paper, deuterium ions from neutral beam injection (NBI) with $E_{\mathrm{NBI}} \approx 100$ keV, injected in the co-B_t/I_p direction ($v_{\|} > 0$), were accelerated to higher energies (up to ~2.5 MeV) in the plasma core using the 3-ion D-(D$_{\mathrm{NBI}}$)-^{3}He radio frequency (RF) scenario [6-7].

A large variety of fast-ion driven MHD modes such as toroidal (TAEs), elliptical (EAEs) and reversed shear (RSAEs) Alfvén eigenmodes [9] with different toroidal mode numbers n, including axisymmetric modes with $n = 0$, were observed in these JET-ILW experiments. The excitation of most of these MHD modes can be explained by resonant wave-particle interactions with a population of ICRF-generated fast D ions. However, the simultaneous observation of $n = -1$ and $n = 0$ modes in the EAE frequency range implies the presence of a fast-ion population in the plasma with a large number of highly energetic counter-passing ions ($v_{\|} < 0$), in addition to having a positive gradient in the particle energy distribution function $\partial f/\partial E > 0$, as a bump on tail [10]. These unusual conditions are consistent with the regular observation of $n = 0$ modes in the EAE frequency range. The combined fast-ion and MHD analysis shows that the ICRF-generated population of fast D ions does not include particles capable of effectively exciting $n = -1$ EAEs.

This, in turn, implies that these modes are driven by another fast-ion population (different from fast D ions) with a substantial fraction of high-energy counter-passing ions. We demonstrate that the fast-ion observations are consistent with the hypothesis that D-^{3}He fusion-born alpha particles drive these modes. For the first time, we propose a theoretical mechanism and provide experimental evidence for a bump-on-tail distribution of fusion born alphas, self-sustained by a periodic modulation of the alpha particle source due to short period sawteeth. Such mechanism unveils that the presence of highly energetic born alpha particles can add extra and unexpected non-linear physical mechanisms to magnetically confined plasmas.

Experimental conditions

The 3-ion D-(D_{NBI})-^{3}He radio frequency (RF) scenario with fast NBI ions as resonant absorbers was used to generate a population of high-energy D ions. The experimental conditions (the vacuum toroidal field in the plasma centre – B_0 = 3.7T, the plasma current – I_p = 2.5MA, the electron density in the plasma centre – $n_{e0} \approx 6\text{-}7\times10^{19}$ m^{-3}), the ion cyclotron RF settings (f = 32.2-33.0 MHz, dipole antenna phasing) and rather large ^{3}He concentrations, $n(^3\text{He})/n_e \approx$ 20-25% were purposely chosen to position the ion-ion hybrid (IIH) layer and thus generate energetic D ions in the plasma core [11]. Accordingly, the cyclotron resonances for thermal D and ^{3}He ions were located off-axis at the high- and low magnetic field side, see Fig. 1(a). The figure shows the RF power deposition, as computed by the TORIC code [12], illustrating that most of RF power is indeed absorbed in a small region in the plasma core by fast D-NBI ions. Figure 1(b) shows an overview of JET pulse #95679 ($P_{NBI} \approx$ 6.9MW, $P_{RF} \approx$ 5.8MW), in which the central electron temperature increased from 3.6 keV during the NBI-only phase to 7.6 keV in the combined ICRF+NBI phase. An efficient generation of high-energy deuterons with ICRF resulted in a strongly increased neutron rate, rising from ~5×10^{14} s^{-1} to ~1.0×10^{16} s^{-1}. The black dotted and red dashed lines in Fig. 1(b) show the D-D neutron and D-^{3}He fusion alpha rates, simulated by TRANSP [13]. A very good agreement between the measured and computed neutron rates was achieved. The bottom panel in Fig. 1(b) shows the time evolution of the ^{3}He concentration, $X[^3\text{He}] = n(^3\text{He})/n_e \approx$ 22%, which was controlled by the real-time feedback system in JET.

In the reported experiments, the fast-ion distribution of the RF accelerated D-NBI ions was controlled by varying the applied ICRF and NBI power, and their ratio. With as little as $P_{RF} \approx$6 MW and $P_{NBI} \approx$ 7-11 MW, rather high D-D neutron (~1×10^{16} s^{-1}) and D-^{3}He alpha rates (~2×10^{16} s^{-1}) were achieved. The time-of-flight neutron spectrometer TOFOR [14] was used to assess the maximum energies of ICRF- accelerated D ions. Neutrons with a time-of-flight > 43 ns were measured by TOFOR corresponding to maximum

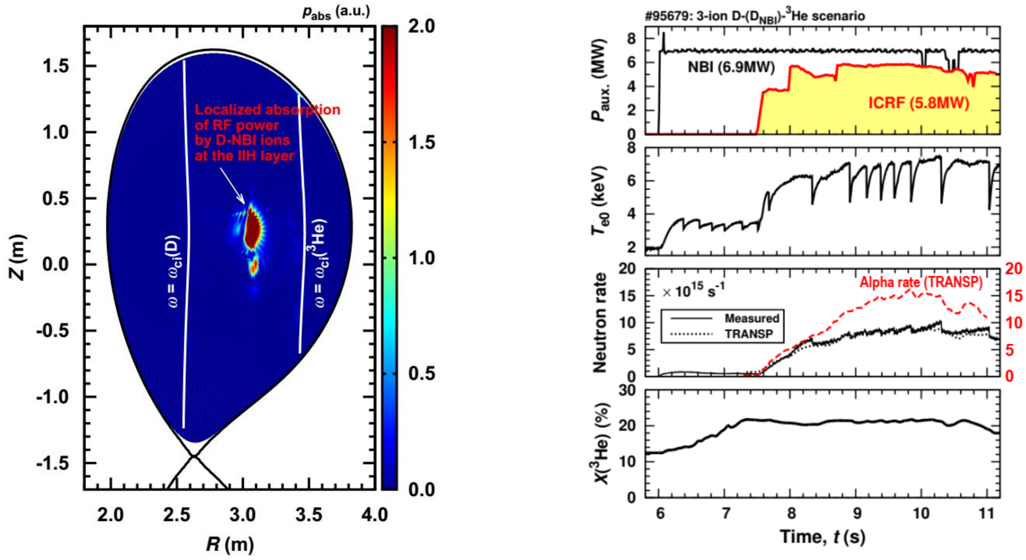

Figure 1. (a) – the poloidal cross-section of the JET tokamak showing the off-axis location of the cyclotron resonances of ^{3}He and D ions (magnetic axis at $R_{MAG} \approx$ 3.0 m) and the core absorption of RF power by fast D-NBI ions, as calculated with the TORIC code. (b) – an overview of JET pulse #95679: the panels show the auxiliary heating power, the central electron temperature, T_{e0}, the measured D-D neutron rate (black solid line) vs. the TRANSP simulation (black dotted line)

and the TRANSP-simulated D-^{3}He fusion alpha rate (red dashed line); the bottom panel shows the ^{3}He concentration controlled by the real-time feedback system.

deuterium energies of about 2.5 MeV. This result is consistent with gamma-ray [15, 16] and fast ion loss detector (FILD) [17] measurements.

Observations of n = –1 and n = 0 modes in the EAE frequency range

Figure 2 shows the time evolution of two other JET pulses, #95666 ($P_{\mathrm{NBI}} \approx 8.1$ MW, $P_{\mathrm{RF}} \approx 5.8$ MW) and #95675 ($P_{\mathrm{NBI}} \approx 6.3$ MW, $P_{\mathrm{RF}} \approx 3.6$ MW) of the same series of fast-ion experiments in D-^{3}He plasmas. In all these discharges the central electron temperature shows repetitive drops, known as sawtooth oscillations. The presence of fast ions in the plasma core has a stabilizing effect on the sawteeth, causing lengthening of their period Δt_{saw} [18, 19]. However, when a certain stability threshold is crossed [20], a sawtooth crash occurs, resulting in a fast drop in T_{e0} and a redistribution of the fast ions in the plasma. The sawtooth dynamics in these experiments is rather complex, depending inter alia on P_{ICRF} and P_{NBI}. The sawtooth period varied over a wide range, from rather short $\Delta t_{\mathrm{saw}} \approx 150$-200 ms up to very long $\Delta t_{\mathrm{saw}} \approx 3.9$ s (a monster sawtooth). A detailed discussion on the sawtooth stabilization is outside the scope of this paper, but as shown below the sawtooth period has a significant influence on the dynamics of the AE modes.

Fast-ion driven MHD modes such as TAEs, EAEs and RSAEs with different toroidal mode numbers, including modes with $n = 0$, were regularly observed in these JET-ILW experiments, see Fig. 3. Furthermore, the axisymmetric $n = 0$ modes were detected. Note the somewhat higher EAE frequencies in #95679 because of the slightly lower plasma density in that pulse. Similarly to past fast-ion experiments with ICRF on JT-60U [21], the behaviour of TAEs and EAEs was influenced by the sawtooth dynamics.

In these JET experiments EAE modes were often observed during phases with short sawteeth, see Figs. 3(b), (d) and (f). In each of these discharges, a monster sawtooth crash facilitated the excitation of EAEs; under these conditions, the delay between the onset of the EAE activities after the monster sawtooth crash was typically ~ 80-100 ms. The observed

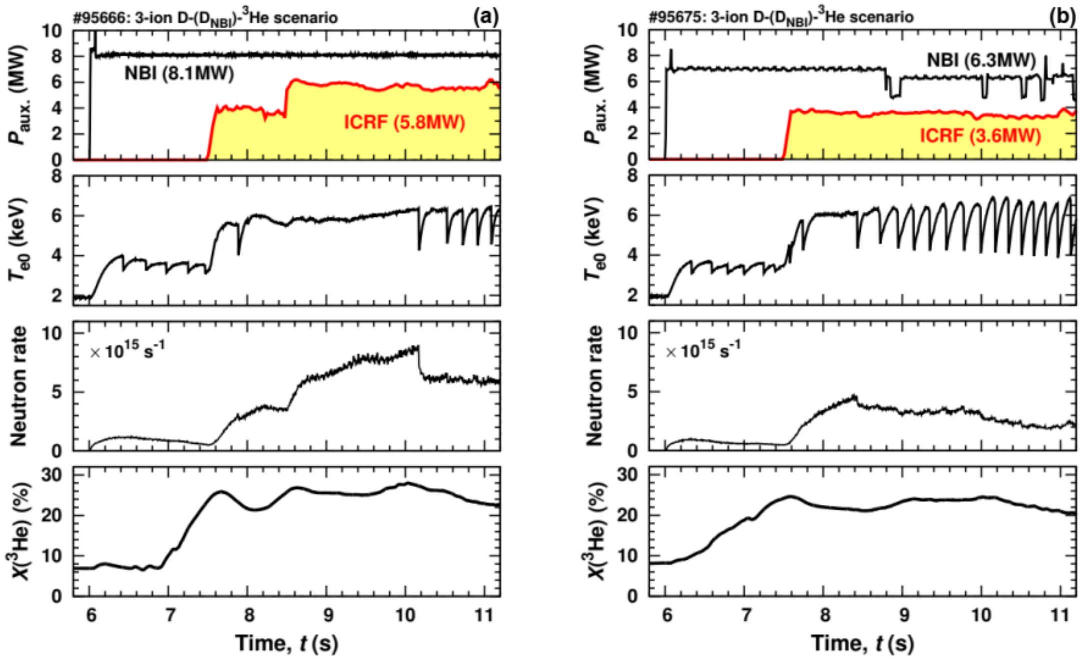

Figure 2. Overview of JET pulses #95666 and #95675 in D-^{3}He plasmas with very different sawtooth dynamics. (a) Pulse #95666 with a monster sawtooth phase, $t = 7.89$-10.17 s ($\Delta t_{\mathrm{saw}} \approx 2.3$s). (b) Pulse #95675 with repetitive short-period sawteeth ($\Delta t_{\mathrm{saw}} \approx 200$-300 ms), following the monster sawtooth crash at $t = 8.43$s ($\Delta t_{\mathrm{saw}} \approx 0.7$s). Note the much lower neutron rate in #95675 due to the reduced ICRF power (3.6 MW).

EAE modes are located at the $q = 1$ surface (q is the magnetic safety factor), as inferred from correlation reflectometer measurements, and consist of two dominant counter-propagating poloidal modes with mode numbers $m_1 = n - 1$ and $m_2 = n + 1$. Note that in the JT-60U experiments mentioned above, EAE modes with only positive toroidal mode numbers $n = 3$-6 were observed [21]. However, in JET D-^{3}He experiments described in this paper, EAEs with lower positive n, as well as $n = 0$ modes and even EAEs with negative toroidal mode numbers were detected. In what follows, we focus our analysis on $n = -1$ and $n = 0$ modes in the EAE frequency range and demonstrate that the simultaneous observation of these modes requires a large number of highly energetic counter-passing ions with a bump-on-tail distribution.

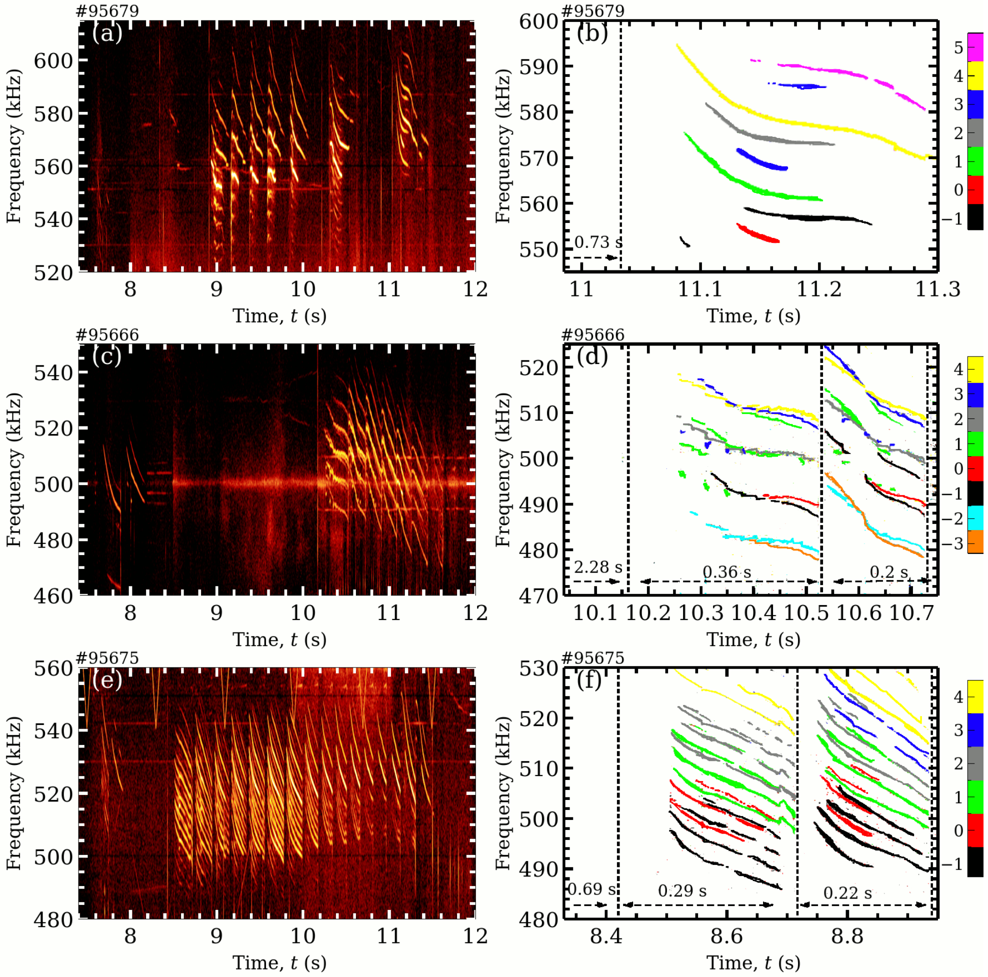

Figure 3. Magnetic spectrograms showing fast-ion driven EAE activities in JET pulses #95679 (a), #95666 (c) and #95675 (e). The vertical dashed lines indicate the timings of the sawtooth crashes. A close-up of the MHD spectra in these pulses shows the presence of $n = -1$ and $n = 0$ modes in the EAE frequency range.

Linear stability analysis

Alfvén eigenmodes are destabilized by energetic ions through the energy transfer between resonant particles and AEs [9]. The necessary condition for resonant wave-particle interaction is given by

$$\omega = n\omega_\varphi + p\omega_\theta, \tag{3}$$

where ω and n are the AE frequency and the toroidal mode number; ω_φ and ω_θ are the toroidal and poloidal orbital frequencies; p is an integer. The destabilization of AEs is only possible when the mode drive by fast ions is sufficiently large and overcomes the mode damping by different mechanisms.

Figure 4 shows the computed efficiency of the resonant wave-particle interaction for the observed $n = -1$ EAE mode at $f \approx 555$ kHz in pulse #95679 (see Fig. 3(b)). The efficiency is obtained by calculating the variance of test-particle energy due to work done by the eigenmode electric field over many wave periods. The computations have been carried out using the HAGIS and MISHKA codes [22, 23] for a typical fixed mode amplitude $\delta B/B = 1\times10^{-5}$ supposing that the $n = -1$ EAE mode is interacting with fast D ions.

From the plotted efficiency of wave-particle interaction in Figure 4, the drive of this mode with a negative toroidal mode number would require the presence of a large population of energetic counter-moving D ions ($v_{||} < 0$) in the plasma. The energy range for fast D ions has been limited to 2.5 MeV, reflecting the experimental observations from the TOFOR neutron spectrometer and other fast ion diagnostics.

The two most prominent power transfer lines in Figure 4 have been labelled to show the corresponding wave-particle resonances identified for different p-numbers in Eq. (3), confirmed by computing the toroidal and and bounce frequencies of the test particles. The computations show that the observed $n = -1$ EAE mode receives energy most effectively from fast counter-passing ions via the $p = 0$ ($\omega = -\omega_\varphi$) and $p = -1$ ($\omega = -\omega_\varphi - \omega_\theta$) resonances. As the toroidal and poloidal orbital frequencies for passing fast ions are given by $\omega_\varphi = v_{||}/R$ and $\omega_\theta = v_{||}/(qR)$ [9], the $n = -1$ EAE mode interact effectively with fast ions at parallel velocities $v_{||} = -\omega R$ and $v_{||} = -\omega R/(1 + 1/q) \approx -\omega R/2$.

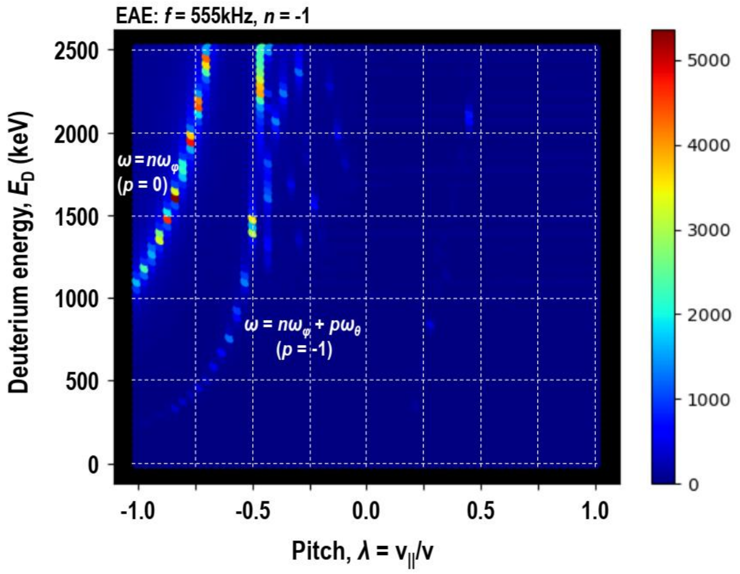

Figure 4. The figure shows the computed strength of resonant wave-particle interaction, supposing that this mode is excited by fast D ions. Excitation of the observed $n = -1$ EAE modes ($f \approx 555$ kHz as in pulse #95679, see Fig. 3(b)) requires a large amount of energetic counter-moving ions ($v_{||} < 0$) in the plasma. These modes are most effectively driven by fast counter-passing ions.

For $f_{\mathrm{EAE}} = 555$ kHz as in pulse #95679 (Fig. 3(b)), one gets $v_{||} \approx -1.1\times10^{7}$ m/s and $v_{||} \approx -5.4\times10^{6}$ m/s, respectively. For fast D ions, these velocities correspond to energies of about 1.2 MeV and 0.3 MeV. Note that weak higher-order wave-particle resonances for $p = -2, -3, \ldots$ are also visible in Fig. 4, but only at negative pitches and at high D energies. An important remark is that while the $p = 2$ resonance can be formally identified for particles with a positive pitch, the energy transfer between these D ions with $v_{||} > 0$ and the $n = -1$ EAE mode is several orders of magnitude less efficient and thus not visible in Fig. 4.

Simultaneously with the observation of the $n = -1$ EAE mode, axisymmetric modes with $n = 0$ were also detected in the same EAE frequency range. These modes were also observed in the past fast-ion experiments with the 3rd harmonic D ICRF acceleration in D-^{3}He plasmas on JET-ILW and the free source of energy to destabilize $n = 0$ modes is provided by positive gradients in the fast-ion energy distribution function, $\partial f / \partial E > 0$ [24]. Thus, the observation of $n = 0$ modes in these JET experiments implies the presence of a population of fast ions with a bump-on-tail distribution. Note that the excitation of $n = 0$ modes does not impose a constraint on the sign of the parallel velocity of resonant ions and these modes can be excited through the energy transfer from fast ions with both $v_{||} < 0$ and $v_{||} > 0$.

In the discussed JET experiments the 3-ion D-(D$_{NBI}$)-^{3}He ICRF scenario with D-NBI ions as resonant absorbers was applied to accelerate these ions to higher energies in the vicinity of the IIH layer in mixed D-^{3}He plasmas [7, 8, 11]. As the NBI system at JET injects fast ions predominantly in the co-direction, i.e. with $v_{||} > 0$ (see the black dashed line in Fig. 5), the developed fast-ion scenario provides a strong selectivity on the sign of the parallel velocity for resonant ions accelerated with ICRF. This is supported by gamma-ray measurements and TRANSP simulations, confirming the preferential generation of highly energetic D ions with positive parallel velocities, $v_{||} > 0$. TRANSP modelling also shows that counter-passing energetic D ions, which are required to drive the observed $n = -1$ EAE modes under these conditions (see Fig. 4), are virtually absent in the fast-ion distribution. Furthermore, the computed pitch-angle averaged distribution function of ICRF-accelerated fast D ions monotonically decreases with energy and does not have a bump-on-tail needed to drive the observed $n = 0$ modes in the EAE frequency range unstable. In the case of a sawtooth, the post-crash neutron rate growth indicates that D ions are in a continuous acceleration with $\partial f_D / \partial E < 0$.

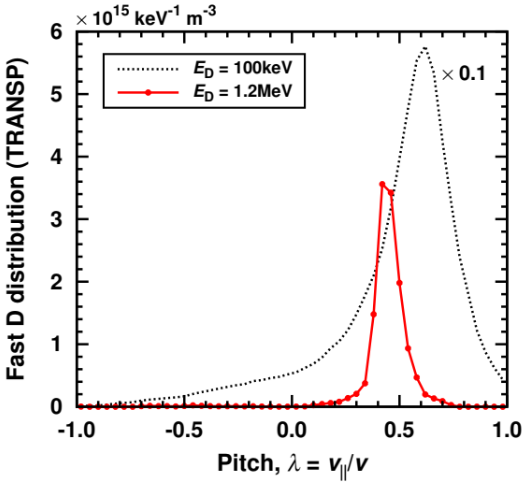

Figure 5. The distribution function of ICRF-accelerated fast D ions at $E_D = 100$ keV (NBI injection energy) and $E_D = 1.2$ MeV as a function of the pitch parameter, computed by the TRANSP code for JET pulse #95679 (see Fig. 1(b)). Note that the fast-ion distribution function at $E_D = 100$ keV was plotted with a multiplication function of 0.1 to illustrate the two distributions on a comparable scale.

These observations imply that the simultaneously observed $n = -1$ and $n = 0$ modes in the EAE frequency range are driven as a result of resonant wave-particle interaction with another fast-ion population present in the plasma. In what follows, we demonstrate that the fast-ion observations are consistent with the hypothesis of D-^{3}He fusion-born alpha particles as the drive for these modes.

Figure 6(a) shows the birth spectrum of alpha particles calculated with the Monte-Carlo code GENESIS [25, 26], using the TRANSP distribution function for fast D ions as input and the extended D-^{3}He fusion cross sections [27]. The fusion-born alpha particles have a rather large broadening in energy space, ranging between ~2 MeV and ~7 MeV. More importantly, the population of alpha particles naturally includes fast ions with a pitch parameter covering the full range from $v_{||}/v = -1$ (counter-passing alphas) to $v_{||}/v = +1$ (co-passing alphas). These are depicted with red solid and dotted lines in Fig. 6(a), respectively.

As follows from the MHD mode analysis presented above, the energy transfer between the counter-passing fast ions with $v_{||} \approx -1.1\times10^7$ m/s and $v_{||} \approx -5.4\times10^6$ m/s and $n = -1$ EAE modes is the most efficient. The map showing the efficiency of the resonant wave-particle interaction for alpha particles as a function of their energy and pitch, is shown in Fig. 6(b). Note that it is rather similar to the one for D ions (Fig. 4), but the corresponding wave-particle resonances are shifted towards higher fast-ion energies as a result of a higher mass of alpha particles. As follows from the figure, counter-passing alphas with energies $E_\alpha \approx 2$ MeV provide the strongest drive for the $n = -1$ EAE mode. These particles are naturally present in the plasma, originating from the D-^{3}He fusion reactions. Note the rather high alpha production rates that were reached in these fast-ion experiments on JET, comparable or even higher than the D-D neutron rates. For example, a D-D neutron rate of ~1×10^{16} s^{-1} was achieved in JET pulse #95679, while the D-^{3}He fusion rate was estimated to be ~2×10^{16} s^{-1} (see Fig. 1(b)).

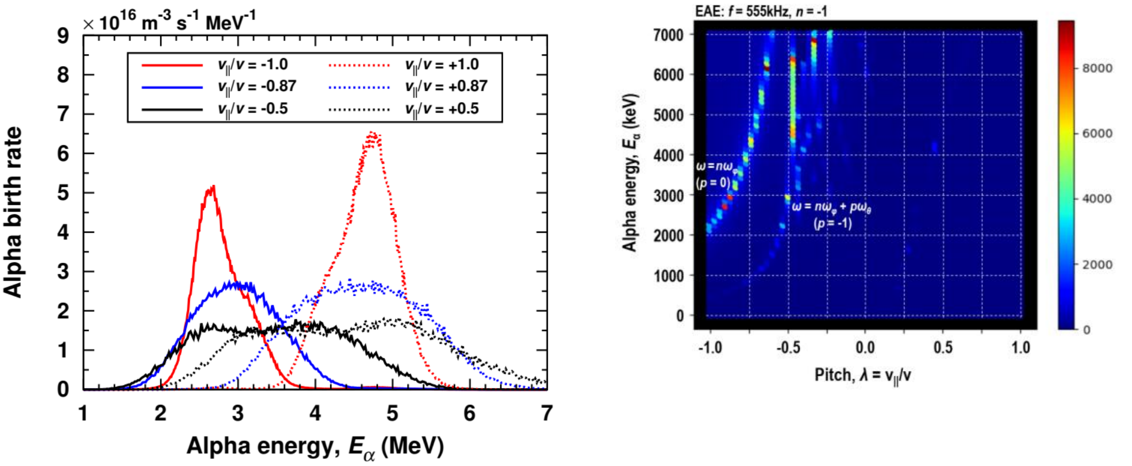

Figure 6. (a) – the birth spectrum of D-^{3}He fusion-born alpha particles has a rather large broadening in energy space 2 MeV < E_α < 7 MeV with a pitch parameter covering the full range from $v_{||}/v = -1$ (counter-passing alphas) to $v_{||}/v = +1$ (co-passing alphas); (b) – computed efficiency of the resonant wave-particle interaction between alpha particles and the observed $n = -1$ EAE modes ($f = 555$ kHz, cf. Fig. 3(b)).

Mechanism to generate a persisting bump-on-tail energy distribution of the D-^{3}He fusion-born alpha particles

The observation of the $n = 0$ mode in the EAE frequency range implies a positive gradient in the particle energy distribution at rather high energies. Yet the steady-state slowing-down distribution of fusion-born alphas decreases monotonically as a function of energy and thus does not feature a bump-on-tail. If the $n = 0$ modes are indeed driven by alpha particles born in D-^{3}He fusion reactions, how can the condition $\partial f_\alpha/\partial E > 0$ be achieved in these fast-ion experiments?

A substantial redistribution of fast D ions as a result of the sawtooth crashes was observed in these experiments. This, in turn, leads to a periodic modulation of the production rate of D-^{3}He fusion-born alpha particles. Note that while the D-D neutron rate increases with the energy of the fast D ions, the energy dependence of the D-^{3}He fusion reactivity has a maximum at $E_D \approx 0.44$ MeV [5]. For example, at $E_D = 0.7$ MeV the D-D neutron rate is lower by 25% as compared to the reactivity rate at $E_D = 1$ MeV, while the alpha rate from the D-^{3}He fusion is larger by ~50%.

Figures 7(a) and (b) show the reconstructed neutron emission profile shortly before and after the monster sawtooth crash at $t = 11.03$ s in JET pulse #95679. The dotted lines show the lines-of-sight of 10 horizontal and 9 vertical neutron camera channels. Following a sawtooth crash, the neutron emissivity from the plasma core is reduced, while an increase in the neutron emissivity is observed in the channels with a line-of-sight further away from the plasma centre. This is illustrated in Fig. 7(c), showing the temporal evolution of neutron counts measured by channels #5 and #6. Note that the monster sawtooth crash leads only to a moderate decrease of ~20% of the total neutron rate.

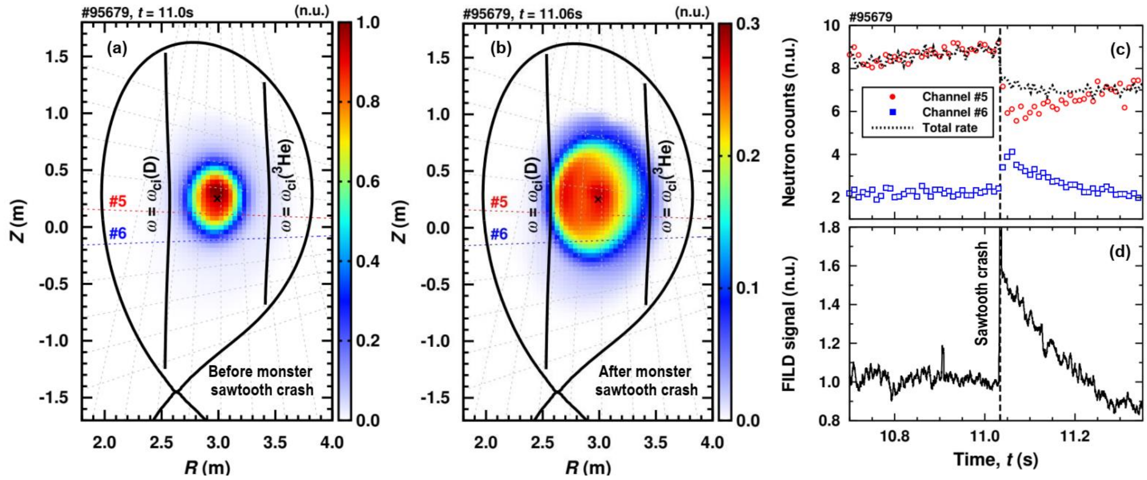

Figure 7. (a) and (b) – the reconstructed neutron emission profile shortly before and after the monster sawtooth crash at $t = 11.03$ s in JET pulse #95679; the dotted lines show the lines-of-sight of the 19 neutron camera channels; (c) – time evolution of the neutron counts during the sawtooth crash (normalised units), as measured by channels #5 and #6 of the neutron camera at JET; (d) – the lost alpha particle signal measured with FILD ($\rho_L \geq 11$ cm, $E_\alpha \geq 4.8$ MeV).

The presence of the confined and lost alpha particles was independently confirmed by the gamma-ray [15, 16] and fast-ion loss detector (FILD) measurements [17]. The former relies on measuring high-energy gamma-rays ($E_\gamma \approx 17$MeV), originating from the ^{3}He(D,γ)^{5}Li reaction, which is a weak branch of the D-^{3}He fusion reaction. However, the diagnostic temporal resolution is not enough to track the detailed fast-ion dynamics during the sawtooth crash.

The FILD system at JET is equipped with 16 photomultipliers, which are providing fast signals ($\Delta t \approx 0.5$ µs) of energetic ions with different energies and pitch-angles escaping from the plasma. Figure 7(d) shows the dynamics of the FILD signal measuring high-energy ions with a Larmor radius $\rho_L \geq 11$ cm ($E_\alpha \geq 4.8$ MeV) and a pitch angle in the range ~55^0-70^0. The loss rate of the alpha particles is increased by ~60% with respect to the level before the sawtooth crash at $t = 11.03$s and the relaxation of the FILD signal takes place on the time scale of ~200 ms. Note also that in pulse #95679 the $n = 0$ mode in the EAE frequency range disappears at $t \approx 11.17$s, as shown in Fig. 3(b).

The mechanism for a persisting bump-on-tail distribution of the resonant fast ions exciting AEs is very similar to the one applied in recent NBI experiments in DIII-D, where short beam modulation periods were applied to create transiently a bump-on-tail velocity distribution [28]. However, in the JET experiments in D-^{3}He plasmas reported here, such a mechanism is self-sustained, since the source rate of fusion-born alpha particles was modulated by the sawtooth period.

In pulses with sawtooth periods shorter than the typical relaxation time for fusion-born alphas, alpha particles did not have enough time to decelerate to thermal energies with the associated monotonically decreasing slowing-down distribution. Thus, the ratio $\Delta t_{\rm saw}/\tau_\alpha^*$ is a characteristic parameter that defines the time evolution of the distribution function of the alphas [29]. To estimate the relevant time scales, we note that the characteristic slowing-down time of alphas is given by:

$$\tau_\alpha^* = (\tau_{\rm se}/3)\ln\left(1 + (E_0/E_{\rm crit})^{3/2}\right), \tag{4}$$

where $\tau_{\rm se}$ is the Spitzer slowing-down time, E_0 and $E_{\rm crit} \approx 41\ T_{\rm e}$ is the initial and the critical energy for alpha particles, at which the rate of loss of energy to the electrons and to the ions is equal. That yields $\tau_\alpha^* \simeq 400\,{\rm ms}$ for alpha particles with birth energies of ~3.6 MeV for the conditions of these JET experiments.

In the reported series of fast-ion experiments in D-^{3}He plasmas, the sawtooth period varied from rather short $\Delta t_{\rm saw} \approx 150$-$200$ ms up to very long $\Delta t_{\rm saw} \approx 3.9$ s, thus providing a scan through the conditions $\Delta t_{\rm saw}/\tau_\alpha^* < 1$ to $\Delta t_{\rm saw}/\tau_\alpha^* \gg 1$. Note that EAE modes in pulses with short-period sawteeth persist during the whole sawtooth period (excluding the period of delayed onset following the crash). Such unusual experimental conditions prevent the creation of a steady-state slowing-down distribution of alpha particles, and, in turn, sustain a bump-on-tail because of the periodic modulation of the alpha particle source.

Summary and conclusions

In this letter we showed that there is a well-defined way to generate conditions favorable for the excitation of AEs with n = –1 and $n = 0$ by fusion-born alpha particles from the D-^{3}He reaction. In such reaction, with the birth energy and kinematics of alpha particles are similar to those released in D-T reactions but with relatively low neutron production, which allows use of fast-ion diagnostics unsuited to the high neutron flux environment of DT experiments.

In our experiments we show that only the fusion-born α-particles can effectively excite $n = -1$ EAEs, which has been confirmed with a linear stability analysis.

For the first time, we propose a theoretical mechanism and provide experimental evidence for the fusion alphas bump-on-tail distribution required to excite $n = 0$ AEs, which is self-sustained by a periodic modulation of the fusion source due to sawtooth crashes.

The demonstration of AEs driven by fusion-born α-particles in D-T plasmas is one of the main objectives in the forthcoming D-T campaign on JET. An extension of the technique presented in this paper is to apply a periodic modulation of NBI power in D-T plasmas with a period shorter than the characteristic slowing-down time of fusion-born alphas.

The Alfvén instability is a significant issue for high-Q operation in ITER. Indeed, the excitation and interaction of fusion-born alpha particles with $n = -1$ and $n = 0$ modes in the EAE frequency range studied in these experiments is important for the development of magnetic fusion reactors since the consequences on fast ion transport and confinement can be substantial.

Acknowledgements.

This work has been carried out within the framework of the EUROfusion Consortium and has received funding from the Euratom research and training programme 2014-2018 and 2019-2020 under grant agreement No 633053 and from the RCUK Energy Programme [grant No EP/T012250/1]. To obtain further information on the data and models underlying this paper please contact PublicationsManager@ukaea.uk . The views and opinions expressed herein do not necessarily reflect those of the European Commission.

References

1. S.E. Sharapov et al 2013 *Nucl. Fusion* **53** 104022
2. R.J. Hawryluk et al., *Phys. Rev. Lett.* **72**, 3530 (1994).
3. JET Team (prepared by P.R. Thomas), *Nucl. Fusion* **39**, 161 (1999)
4. J.H. Weisen et al, "The scientific case for a JET D-T experiment", *AIP Conference Proceedings* **1612**, 77 (2014); https://doi.org/10.1063/1.4894028
5. H.S. Bosch and G.M. Hale, *Nucl. Fusion* **32** 611 (1992)
6. Ye.O. Kazakov et al., *Nat. Phys.* **13** 973 (2017)
7. J. Ongena et al., *EPJ Web Conf.* **157**, 02006 (2017)
8. Ye.O. Kazakov et al., *Nucl. Fusion* (2020), in press; https://doi.org/10.1088/1741-4326/ab9256
9. W.W. Heidbrink, *Phys. Plasmas* **15**, 055501 (2008)
10. H. L. Berk, B. N. Breizman and M. Pekker, *Phys. Plasmas* **2** (1995) 3007
11. M. Nocente et al., "Generation and observation of fast deuterium ions and fusion-born alpha particles in JET D-^{3}He plasmas with the 3-ion radio frequency heating scenario", submitted to *Nucl. Fusion* (2020)
12. M. Brambilla, *Plasma Phys. Control. Fusion* **41**, 1 (1999)
13. R.V. Budny, *Nucl. Fusion* **34**, 1247 (1994).
14. J. Eriksson et al., *Plasma Phys. Control. Fusion* **61**, 014027 (2019)
15. V.G. Kiptily et al., *Plasma Phys. Control. Fusion* **48**, R59 (2006)
16. M. Nocente et al 2020 *Plasma Phys. Control. Fusion* **62** 014015
17. V.G. Kiptily et al, 2018 *Nucl. Fusion* **58** 014003
18. R.B. White et al., *Phys. Rev. Lett.* **60**, 2038 (1988)
19. I.T. Chapman et al., *Plasma Phys. Control. Fusion* **49** B385 (2007)
20. F. Porcelli et al., *Plasma Phys. Control. Fusion* **38**, 2163 (1996)
21. G.J. Kramer et al., *Nucl. Fusion* **41**, 1135 (2001)
22. S.D. Pinches et al., *Comput. Phys. Commun.* **111**, 133 (1998)
23. A.B. Mikhailovskii et al., *Plasma Phys. Rep.* **23**, 844 (1997)
24. H.J.C. Oliver et al., *Phys. Plasmas* **24**, 122505 (2017)
25. M. Nocente, in *Neutron and gamma-ray emission spectroscopy as fast ion diagnostics in fusion plasmas*, PhD thesis, Università degli Studi di Milano-Bicocca (2012)
26. M. Tardocchi et al., 2011 *Phys. Rev. Lett.* **107** 205002
27. M. Nocente et al, *Nucl. Fusion* **50** (2010) 055001

28. M. Van Zeeland et al, presentattion at the *16th IAEA TM on Energetic Particles in Magnetic Confinement Systems*, Shizuoka, Japan, Sept. 3-6, 2019; https://conferences.iaea.org/event/185/contributions/14962/attachments/8141/10805/mvz_iaea_tm_talk_beam_mod_43_pub.pdf
29. V.G. Kiptily et al, 2004 *Phys. Rev. Lett*. **93** 115001